



Spectroscopic, optical, mechanical, and electrical characterization of PEO/PVA incorporated by GO nanopowder

Nuha Al-Harbi¹

Received: 20 December 2023 / Accepted: 1 January 2024 / Published online: 30 January 2024
© The Author(s), under exclusive licence to Springer Science+Business Media, LLC, part of Springer Nature 2024

Abstract

In this study, polyethylene oxide (PEO)/polyvinyl alcohol (PVA) nanocomposite films incorporated with different concentrations of graphene oxide nanoparticles (GO NPs) were fabricated and characterized. The nanocomposites were characterized by XRD, FT-IR, optical spectroscopy, tensile testing, and electrical conductivity. The X-ray results suggest that adding of GO to PEO/PVA improves their compatibility and causes a decrease in the degree of crystallinity. The FT-IR spectra suggest the creation of stronger hydrogen bonds between the PEO/PVA polymeric chains and the GO as a filler. The absorbance spectra show increased UV-vis absorbance after adding GO nanopowders. The Tauc equation was used to calculate the optical band gap (E_g) which increased after adding GO nanopowders. The mechanical and electrical properties of the samples are also studied. The results reveal that incorporating GO led to an overall reinforcing effect on the mechanical and dielectric properties. Moreover, the frequency of the electric field, the concentrations of the GO NPs, and interfacial interactions between GO and the polymer matrix were identified as important factors that can influence the dielectric property of the nanocomposite. In addition, the relationship between Z' and Z'' of the PEO/PVA-GO films provided important insights into the electrical behavior. The best PEO/PVA-GO nanocomposite sample shows potential for various applications, including electronics, battery energy storage and engineering field.

Keywords PEO/PVA · GO nanopowders · XRD · FT-IR · Mechanical testing · Dielectric permittivity

✉ Nuha Al-Harbi
nfhariby@uqu.edu.sa

¹ Physics Department, Faculty of Applied Sciences, Umm Al-Qura University, Makkah, Saudi Arabia

1 Introduction

Polymer nanocomposites consist of a polymer matrix with small nanoparticles dispersed throughout the matrix at nanoscale levels as metal oxides and graphene oxide (Elashmawi and Al-Muntaser 2021; Tanaka et al. 2004; Abdelghany et al. 2023; Huang et al. 2020). Polymer nanocomposites exhibit several unique properties not found in traditional polymers or inorganic materials. Some of these properties of polymer nanocomposites include enhanced mechanical, improved thermal, and electrical properties (Althubiti et al. 2022; Al-Farraj et al. 2018; Sharma et al. 2018). Polymer nanocomposites can potentially find applications in diverse fields owing to their unique properties and characteristics (Chen et al. 2018; Ibrahim et al. 2023). The dispersion of the nanoparticles in the polymer blends is also an important factor that affects the properties of the nanocomposite (Hamed et al. 2022; Menazea et al. 2020; Sreekanth et al. 2019).

Polyethylene oxide (PEO) is a water-soluble polymer with excellent film-forming properties. When combined with graphene oxide, PEO can act as a dispersant, improving the dispersion and stability of graphene oxide in water-based solutions (Olabi et al. 2021). Polyvinyl alcohol (PVA) is widely used in various applications due to its unique properties (Mousa 2022; Aassar et al. 2023; Alibwaini et al. 2021). PVA is known for its excellent film-forming properties, this attribute makes polymer nanocomposites suitable and able to be employed for various applications, like coatings, adhesives, and packaging materials. It is also known for its high tensile strength, flexibility, and barrier properties, making it useful in textiles, paper, and food packaging applications. PVA also can form strong hydrogen bonds, which gives it excellent mechanical properties and makes it useful in applications such as textiles and paper. Its ability to form hydrogen bonds also allows it to act as a stabilizing agent in emulsions and suspensions.

PEO/PVA blend is a combination of two water-soluble polymers, PEO and PVA, which exhibits improved mechanical properties compared to individual polymers. The blend is formed by mixing PEO and PVA in a solvent (Elashmawi et al. 2022). The PEO/PVA blend combines the unique properties of both polymers, including excellent film-forming properties, high tensile strength and good compatibility. The blend exhibits better mechanical properties than individual polymers.

Graphene oxide (GO) is a two-dimensional material that is derived from graphene through a process known as oxidation (Aparna Nair et al. 2023; Oh et al. 2023; Zankana et al. 2023; Elashmawi et al. 2014). GO exhibits several unique properties that make it useful in various applications. GO has high mechanical strength and electrical properties. In energy storage, the high conductivity and surface area of GO make it suitable for use as an electrode material in batteries.

The latest research in polymeric nanocomposite films involves incorporating graphene oxide (GO) nanopowder into the PEO/PVA polymer blend as a good example of a homogeneous and compatible polymer. This combination offers exciting possibilities to enhance the properties of the composite material as GO nanopowder acts as a strengthening agent, improving structural properties, mechanical strength and good electrical conductivity. In addition, the unique interfacial interactions between PEO, PVA, and GO NPs contribute to enhanced compatibility and dispersion. This newest PEO/PVA-GO nanocomposite shows great potential for various applications, including electronics, energy storage, and engineering.

The work aims to prepare and characterize PEO/PVA nanocomposites, incorporated with graphene oxide nanoparticles (GO NPs) using the casting method. The nanocomposites will be characterized using various techniques. The mechanical and electrical properties of the nanocomposites are studied. The results bring to light the potential of GO as a reinforcing and enhancing agent for PEO/PVA-GO nanocomposites in different applications.

2 Experimental

2.1 Materials

Polyethylene oxide (PEO) used in this study was sourced from ACROS (New Jersey, USA) and had a molecular weight of 900,000 g/mol. Polyvinyl alcohol (PVA) with a molecular weight of 14,000 g/mol was procured from E-Merck (Germany). The nanopowders of Graphene oxide (GO) were provided by Sigma-Aldrich.

To prepare PEO/PVA-GO nanocomposites, three grams of PEO and one gram of PVA were dissolved separately in distilled water at 25 °C under constant stirring for 4 h. Various contents (0.2, 0.4, 0.6, and 0.8 wt%) of graphene oxide (GO) were added to the PEO/PVA blend solution and sonicated for 4 h to ensure complete dispersion of GO in the solution. The PEO/PVA blend solution containing GO was mixed under constant stirring for about 10 min. Afterward, the PEO/PVA-GO nanocomposite solution was poured into a petri dish. Then, it was left to air-dry at 48 °C for 36 h to remove solvent and moisture. The PEO/PVA-GO nanocomposite samples were obtained with thickness $\sim 200 \pm 5$ μm .

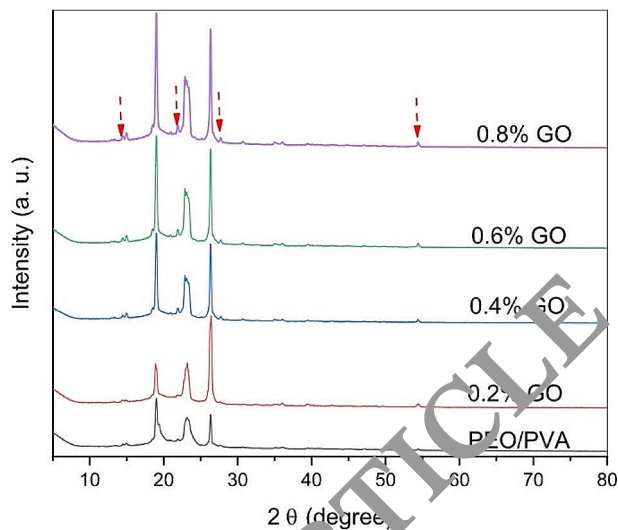
X-ray diffraction (XRD) scans were measured using a DIANO corporation instrument that was equipped with a $\text{CuK}\alpha$ radiation source ($\lambda = 1.540$ Å). The tube was operated at 15 kV, and the Bragg angle $2\theta = 10$ – 80° . The FT-IR spectrometer with a single beam was used in the measurement using a JASCO FT-IR-430 in the range of wavenumber 4000 – 400 cm^{-1} . A Jasco 630 spectrophotometer was employed to measure the absorbance UV-Vis spectra in the 190 – 1000 nm range. The Lloyd LRX5K mechanical testing machine was a computer controlled machine used for mechanical testing. The samples were subjected to tensile forces during the testing process at a 2 mm/min rate. An LCR meter was employed to measure the samples' dielectric properties and electrical conductivity, with AC measurements taken over a frequency range spanning 0.1 Hz to 10 MHz.

3 Results and discussion

3.1 X-ray diffraction

The X-ray diffraction (XRD) of the PEO/PVA blend doped with varying concentrations of GO NPs, within the scanning range of $2\theta = 5^\circ$ to 80° , is depicted in Fig. 1. The most prominent peak in the XRD spectrum of PEO is typically located at around $2\theta \sim 19.09^\circ$. This peak corresponds to the (110) crystal plane of the PEO crystal lattice and is used to calculate the interplanar spacing, or d-spacing, of the crystal structure. The d-spacing of PEO is typically around 4.5 Å, which is consistent with the distance between adjacent polymer chains in the crystalline regions. The diffraction peaks of PEO occur at 2θ values of 19.09° , 23.05° , and

Fig. 1 The X-ray diffraction (XRD) patterns of the PEO/PVA blend doped with varying concentrations of GO NPs



26.4°, which correspond to the (120), (112), and (222) crystal planes (hkl), respectively (Basfer 2023; Huang et al. 2017).

The XRD spectrum of PVA typically shows a broad, diffuse peak centered on $2\theta = 20\text{--}25$ degrees. This peak is characteristic of the amorphous region of the PVA polymer and indicates that PVA does not have a well-defined crystal structure in the amorphous region. The broadness of the peak suggests that the polymer chains are randomly oriented and disordered in the amorphous region.

The XRD spectrum of the PEO/PVA polymer blend typically shows a combination of the characteristic peaks of both polymers. The PEO peaks are typically sharp and well-defined, indicating the presence of well-defined crystalline regions, while the PVA peaks are broader and less well-defined, indicating a more disordered structure. The most prominent peak in the XRD spectrum of the PEO/PVA blend typically corresponds to the (110) crystal plane of the PEO crystal lattice, which calculates the crystal structure's interplanar spacing, or d-spacing. In addition to the (110) peak, the XRD spectrum of the PEO/PVA blend may also show peaks corresponding to the crystalline regions of both polymers.

The XRD spectrum of a PEO/PVA-GO nanocomposite typically shows a combination of the characteristic peaks of the polymer matrix and graphene. The peaks of the polymer matrix are typically sharp and well-defined, while the peaks of GO are broad and less well-defined. In addition to the (110) peak, the XRD spectrum of the PEO/PVA-GO nanocomposite may show additional peaks corresponding to graphene.

The XRD diffraction of pure graphite shows a strong peak at $2\theta = 26.5^\circ$, corresponding to the (002) plane of the graphite crystal lattice. This peak indicates the highly ordered stacking of graphene layers in graphite, with a d-spacing of 3.5 Å. A small peak is also observed at $2\theta = 54.5^\circ$, corresponding to the (004) plane with a d-spacing of 1.9 Å. The XRD of GO shows a peak at $2\theta = 13.9^\circ$ (Parvathi et al. 2023; Sappani Muthu et al. 2022), that disrupts the highly ordered stacking of graphene layers. The observed peak corresponds to a d-spacing of 8.9 Å, significantly greater than the d-spacing of pure graphite.

The XRD spectrum of PEO/PVA-GO nanocomposites may show an increase in the intensity of the polymer blend peaks with the addition of GO. The degree of these changes can offer insights into the interaction between the nanocomposites, including the level of exfoliation or aggregation of GO within the PEO/PVA material. The results suggest that introducing GO to a PEO/PVA polymer blend enhances the interconnectivity between the polymeric chains. This is due to the presence of bonds in GO interacting with the polymeric chains, which enhances the compatibility of the samples. Additionally, the existence of GO may reinforce the interaction between the PEO/PVA blend and GO, causing a decrease in the crystalline phase of PEO in the nanocomposites. This may cause an increase in the conductivity of the nanocomposites.

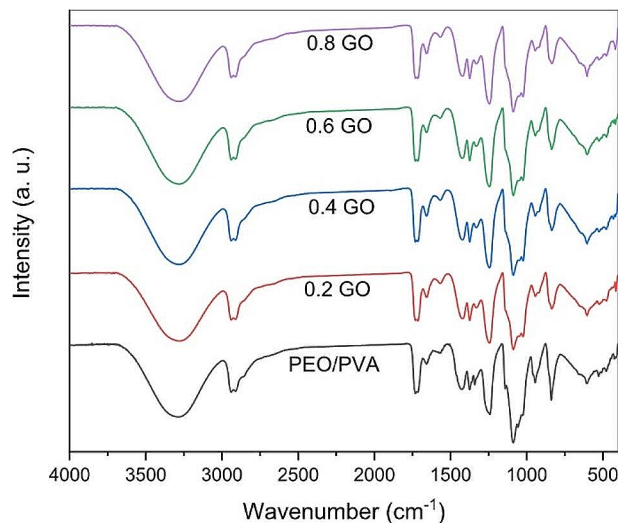
3.2 FT-IR

The FT-IR spectra of the PEO/PVA blend doped with varying concentration of GO NPs are depicted in Fig. 2.

The FT-IR spectrum of PEO typically shows several characteristic bands, corresponding to various functional groups on the polymer blend chain. The FT-IR spectrum of PEO exhibits a band centered at 3303 cm^{-1} , which corresponds to the O-H stretching vibrations of any residual solvent present in the sample. The primary bands of the FT-IR spectrum are generally situated around 3909 cm^{-1} , which corresponds to the C-H stretching vibrations of the polymer backbone, and within the range of $1250\text{--}1080\text{ cm}^{-1}$, due to the C-O. Additionally, the band centered at 1736 cm^{-1} corresponds to the C=O stretching vibrations of any residual ester end groups in the sample. The FT-IR spectrum also shows CH₂ scissoring mode at 1464 cm^{-1} , CH₂ wagging mode at 1538 cm^{-1} , and CH₂ twisting mode at 1246 cm^{-1} .

Furthermore, PEO's characteristic C-O-C stretching absorption bands are present at 1141 cm^{-1} and 1092 cm^{-1} . The spectrum displays CH₂ rocking modes at 942 cm^{-1} and 832 cm^{-1} and a C-O-C bending mode at 526 cm^{-1} . The formation of these end groups during the synthesis or processing of PEO can potentially influence the properties of the blend. The FT-IR spectrum of PVA may exhibit bands within the range of $3200\text{--}3600\text{ cm}^{-1}$, which

Fig. 2 The FT-IR spectra of the PEO/PVA blend doped with varying concentration of GO NPs



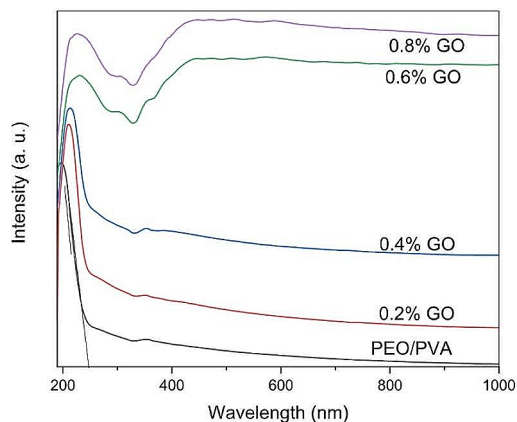
correspond to the O-H stretching vibrations of the hydroxyl groups present in the polymer chain. This band is usually broader than the C-O stretching band and may display splitting or shifting. The FT-IR spectrum of pure PVA displays characteristic absorption peaks at 3580, 2974, 1741, 1570, 1460, and 845 cm^{-1} . The absorption bands at 1741 and 1570 cm^{-1} correspond to the stretching vibrations of C=O. The 1460 cm^{-1} band is associated with the bending vibrations of the C-H group. The absorption bands at 1400 and 1300 cm^{-1} are attributed to the wagging vibrations of C-H and CH_2 , respectively. The band at 1140 cm^{-1} is present due to the stretching vibrations of C-O-C and C-O, while the bands at 910 and 838 cm^{-1} are due to the stretching vibration mode of C-C and out-of-plane bending in O-H, respectively. The primary bands of GO are typically observed within the range of 3000–3600 cm^{-1} , which is assigned to the O-H function groups, and within the range of 1700–1800 cm^{-1} , which is attributed to the C=O carboxyl groups.

The FT-IR spectrum of PEO/PVA-GO nanocomposites shows characteristic bands of all three materials. The bands of the polymer backbones are generally found within the range of 2880–3300 cm^{-1} , corresponding to the C-H stretching modes, while the ether and alcohol groups in the polymer chains typically exhibit bands in the range of 1100–1300 cm^{-1} , corresponding to the C-O stretching modes. The FT-IR spectrum of the PEO/PVA-GO nanocomposites may also exhibit bands in 1600–1700 cm^{-1} , due to the C=O mode of carboxylic groups on the surface of the GO. These bands can provide insights into the extent of functionalization and oxidation of the GO in the nanocomposites. Additionally, the PEO/PVA-GO nanocomposites' FT-IR spectrum may show bands that indicate the interaction between the GO and the polymer chains. The intensity and position of the C-O stretching band can provide information about the degree of hydrogen bonding between the GO and the PEO and PVA chains.

3.3 Optical study

The absorbance spectra of PEO/PVA incorporated by different contents of GO are shown in Fig. 3. PEO and PVA are transparent polymers that absorb minimally in the visible region. Hence, the PEO/PVA blend is also expected to be transparent, with low absorbance in the visible range. An absorption band is observed at around 198 nm due to π - π^* transitions of

Fig. 3 The absorbance UV-Visible spectra of PEO/PVA-GO nanocomposites



the C-O bonds and the absorbance is around 248 nm due to $n-\pi^*$ transitions of the C=O bonds. In the PEO/PVA blend, these absorption bands will likely overlap and broaden, resulting in a broad absorbance shoulder in the UV region (below 285 nm). The absorbance in the visible region (above 390 nm) is likely to remain very low, indicating the transparency of the blend films. However, the absorbance may increase gradually with wavelength due to Rayleigh scattering effects.

Several changes in the absorbance spectra could be observed when the PEO/PVA blend is doped with GO. Absorbance is likely to increase across the UV-vis region due to light absorption by the GO sheets. GO exhibits strong light absorption across the UV-vis and near-IR regions due to its extensive system of π -conjugated bonds.

The absorption band is attributed to $\pi-\pi^*$ transitions of aromatic C-C bonds. This band is characteristic of GO and is typically used to determine the concentration of GO in a solution. A shoulder around appears due to $n-\pi^*$ transitions of C=O groups on GO indicating the extent of oxidation of GO. The absorption bands broaden and red-shift with an increasing degree of oxidation of GO due to introducing more functional groups. The Tauc method determines the optical band gap (E_g). The absorbance coefficient (α) using Beer's law is given from:

$$\alpha = \frac{2.303A}{d} \quad (4)$$

where A is the absorbance and d is sample thickness.

To calculate the bandgap (E_g) of a material based on its absorption spectrum in high absorption zones, where the material absorbs a significant amount of light, Tauc's equation can be used. Tauc's equation relates the absorption coefficient (α) of a material to its bandgap energy (E_g) and a constant (A) (Raghuvanshi et al. 2012; Elashmawi and Menazea 2019):

$$\alpha h\nu = A(h\nu - E_g)^n \quad (5)$$

where α is the absorption coefficient, $h\nu$ is the photon energy of the incident light, and n is a constant that depends on the nature of the electronic transition involved ($n = \frac{1}{2}$ for direct bandgap materials and $n=2$ for indirect bandgap materials).

Figure 4 shows the plotting between $(\alpha h\nu)^{1/2}$ as a function of $h\nu$ for PEO/PVA nanocomposites. Extrapolating the linear portion of the resulting curve to the x-axis (i.e., $\alpha h\nu=0$) can determine the direct bandgap energy (E_g). For GO, the optical band gap is typically in the range of 2.5–3.1 eV. In PEO/PVA-GO, the band gap will decrease due to the quantum confinement effect from 5.81 eV for PEO/PVA blend to 5.66 eV for PEO/PVA doped 0.8 wt%. The gradual decrease in E_g depends on the ratio of GO. As reduction proceeds, E_g will decrease due to the restoration of sp^2 domains.

3.4 Mechanical study

The mechanical properties of PEO/PCA-GO nanocomposites with different graphene oxide (GO) concentrations are evaluated using a universal testing machine. The purpose of the testing is to explore how the treatment of GO impacts the mechanical properties of the

Fig. 4 The relation between $(\alpha h\nu)^{1/2}$ as a function of $h\nu$ of PEO/PVA-GO nanocomposites

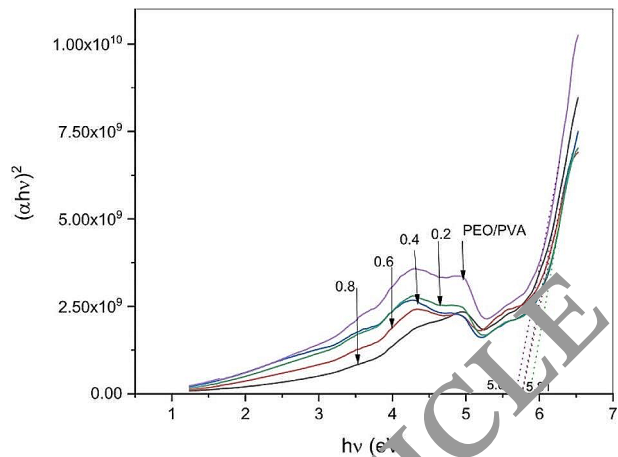
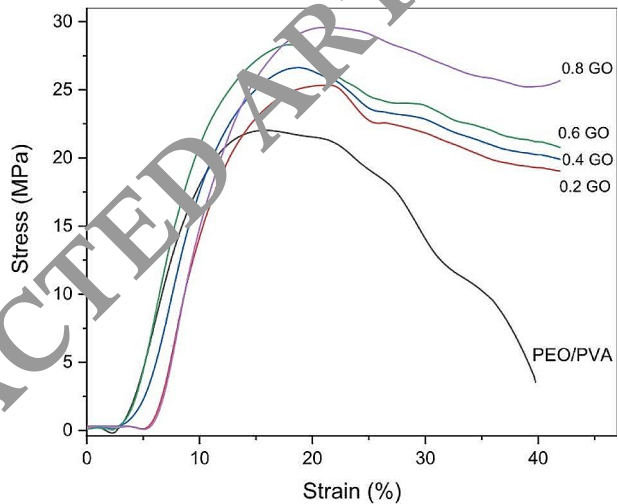


Fig. 5 The relation between tensile stress–strain behavior of the PEO/PVA blend doped with varying concentrations of GO NPs



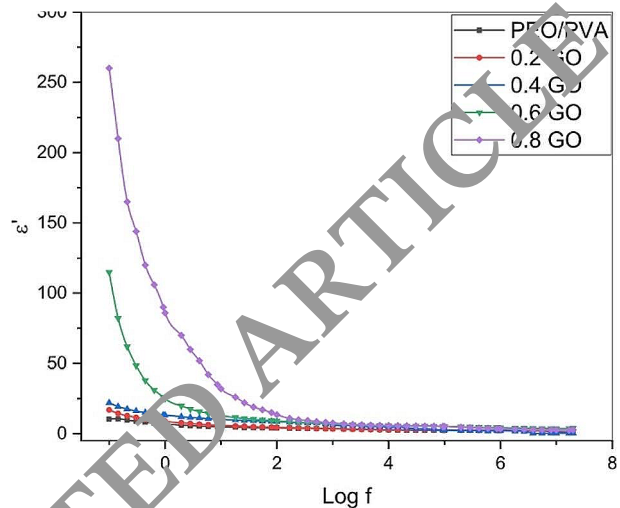
prepared nanocomposites. The universal testing machine is a frequently employed tool for evaluating the mechanical characteristics of materials, such as tensile strength, elastic modulus, and strain to failure.

The elastic modulus is calculated as the slope of the linear region of the stress-strain curve, often referred to as the “elastic” or “linear” region. The elastic modulus represents the stiffness of the material and its ability to resist deformation under an applied load. The tensile strength is the highest stress value obtained from the stress-strain curve, attributed to the point where the material fractures or breaks. The strain to failure is the maximum strain value obtained from the stress-strain curve, attributed to the point where the material fractures or breaks. The strain to failure provides an indication of the ability of the material to deform before it fractures or breaks.

Figure 5 shows the stress-strain curve of PEO/PVA-GO nanocomposites with different contents of graphene oxide, specifically at 0.2, 0.4, 0.6, and 0.8 GO wt% of composite. The

Table 1 Elastic modulus, Tensile strength, and Strain to failure determined from stress-strain curve relations

Samples	Elastic Modulus (Mpa)	Tensile Strength (Mpa)	Strain to failure (%)
PEO/PVA	90	16.61	34.77
0.3	286	20.28	40.95
0.4	289	26.42	40.46
0.6	291	28.38	41.44
0.8	306	29.07	40.95

Fig. 6 The relation between dielectric constant (ϵ') and Log f of the PEO/PVA blend doped with varying concentrations of GO NPs

findings illustrated in the figure and Table 1 suggest that the inclusion of GO resulted in a strengthening effect on the tensile stress, elastic modulus, and strain to failure of the PEO/PVA-GO samples.

The results indicate that increasing GO filler led to an increase in the elastic modulus. This can be attributed to the orientation of GO within the sample during tensile testing, which resulted in improved reinforcement. Once the sample fractured, the reinforcing fillers remained intact, demonstrating the significant improvement in adhesion between the GO and matrix that was achieved through polymer grafting from the surface of GO.

3.5 Dielectric study

Figure 6 displays the relation between the dielectric constant (ϵ') and Log (f) of the PEO/PVA-GO nanocomposites at room temperature. The dielectric constant of the PEO/PVA-GO nanocomposite is an important electrical property that several factors can influence (Zhou et al. 2013; Hemalatha et al. 2015). Adding GO NPs to the PEO/PVA blend can enhance the nanocomposite's dielectric constant due to GO's high permittivity. The permittivity of GO is much higher than that of PEO and PVA, which can increase the dielectric constant. Moreover, the interfacial interactions between GO and the blend generate interfacial dipoles, which result in an increase in the dielectric constant after the addition of GO. At low frequencies, the dielectric constant is mainly determined by the polarization of the polymer matrix and the interfacial polarization between the polymer matrix and the GO

NPs (Elashmawi et al. 2022, 2023). However, at high frequencies, the dielectric constant is primarily governed by the orientation of the dipoles in the material and the conductivity of the polymer matrices.

The dielectric constant of PEO/PVA-GO nanocomposites is an important electrical property that several factors, including the composition and structure of the nanocomposite, can influence. The addition of GO NPs to the PEO/PVA blend can enhance of ϵ' due to the high permittivity of GO NPs. The permittivity of GO is much higher than that of PEO and PVA, which can increase the nanocomposite's overall dielectric constant.

The frequency of the electric field is another important factor that can affect the dielectric constant of the nanocomposites. At low frequencies, the dielectric constant is mainly governed by the polarization of the polymer matrix and the interfacial polarization between the polymer matrix and the GO NPs. At high frequencies, however, the dielectric constant is dominated by the orientation of the dipoles in the material and the conductivity of the polymer matrix. The dielectric constant of PEO/PVA-GO nanocomposites can also be affected by the concentration of GO NPs. At low concentrations. The dielectric constant may not change significantly with the addition of GO. Still, the dielectric constant can increase significantly at higher concentrations due to the formation of conductive networks between the GO NPs (Elashmawi et al. 2017).

Figure 7 illustrates the relation between dielectric loss (ϵ'') and Log f of the PEO/PVA blend doped with varying concentrations of GO NPs at room temperature. Dielectric loss (ϵ'') refers to the energy loss in a material when subjected to an alternating electrical field and is proportional to Z'' . The logarithm of frequency (Log f) is a metric that describes how the material's dielectric properties are affected by frequency changes (Alshammari 2022; Ahamad and Ahmed 2023). The relationship between ϵ'' and Log f of the PEO/PVA blend doped with GO NPs will depend on various factors, such as the concentration and size of the NPs and the characteristics of the polymer matrix. For example, increasing the concentration of GO NPs causes an increase in ϵ'' with frequency. The shape of the ϵ'' vs. Log f curve can provide information about the mechanism of charge transport in the material. For example, a peak in the curve at a certain frequency may indicate the presence of a relaxation

Fig. 7 The relation between dielectric loss (ϵ'') and Log f of the PEO/PVA blend doped with varying concentrations of GO NP.

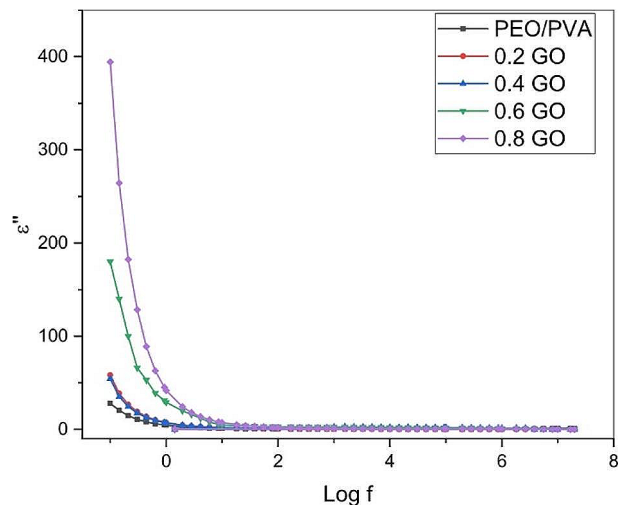
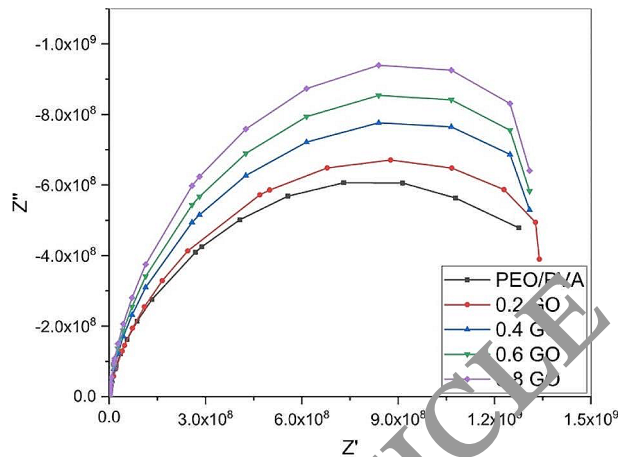


Fig. 8 The plot between the real component (Z') and imaginary component (Z'') of the PEO/PVA blend doped with varying concentrations of GO NPs



process, such as the movement of the PEO/PVA chains or the polarization of GO in response to the electrical field.

The relationship between the real (Z') and imaginary (Z'') components can provide important insights into the electrical properties of the composite material. Figure 8 shows the plot between Z' and Z'' of the PEO/PVA blend doped with varying concentrations of GO NPs. The real component (Z') of the impedance represents the resistance of the material to the flow of electrical current, while the imaginary component (Z'') represents the capacitance and/or inductance of the material. When a material is subjected to an alternating electrical field, these components can change in response to the frequency of the field. This can reveal information regarding the electrical properties of the nanocomposites. The observed relationship between Z' and Z'' of the PEO/PVA blend doped with GO NPs will depend on various factors and the characteristics of the polymer matrix. Finally, increasing GO NP concentration can increase the material's conductivity. This, in turn, can cause the Z' component to decrease and the Z'' component to increase.

4 Conclusion

The conclusion of this work indicates that the XRD of pure GO shows a highly ordered stacking of graphene layers with a d-spacing of 3.5 Å and a more disordered and amorphous structure with a d-spacing of 8.9 Å. The XRD spectrum of a PEO/PVA-GO nanocomposite shows a combination of the characteristic peaks of the polymeric matrices and graphene, with changes in the intensity indicating the interaction between graphene and the polymer blend. This leads to a reduction in the degree of crystallinity and a decrease in the size of the crystalline regions. The FT-IR spectrum of the PEO/PVA-GO nanocomposites exhibit bands in 1600–1700 cm^{-1} , due to the C=O mode of carboxylic groups on the surface of the GO. The UV-vis absorbance increased in the absorbance spectra after adding GO. The optical band gap values (E_g) were decreased due to the quantum confinement effect from 5.81 eV for PEO/PVA blend to 5.66 eV for PEO/PVA doped 0.8 wt%. The mechanical study revealed that incorporating GO causes a reinforcing effect on the tensile stress, elastic modulus, and failure of the nanocomposites. The frequency of the electric field and concentration of GO

NPs were identified as important factors that can influence the dielectric properties of the nanocomposite. The results highlight the potential of GO as a reinforcing and enhancing agent for PEO/PVA-GO nanocomposites in various applications.

Acknowledgements

Author contributions Nuha Al-Harbi: supervised the findings of this work, writing the original draft, reviewing, and editing. Conceived the presented idea and conducted the experiment, analysis, and investigation. Discussed the results and contributed to the final manuscript.

Funding No funding was obtained for this study.

Data availability No datasets were generated or analysed during the current study.

Declarations

Conflict of interest The author declares that there is no conflict of interest regarding the publication of this paper.

References

- Abdelghany, A.M., Elashmawi, I.S., Al-Shamari, A.A., Al-Farraj, H.: Dielectric behavior and AC conductivity of PEO/CMC polymer blend incorporated with gold nanoparticles produced by laser ablation. *J. Mater. Sci. Mater. Electron.* **34**, 1–18 (2023). <https://doi.org/10.1007/s10854-022-09797-z>
- Ahamad, T., Ahmed, A.S.: Influence of graphene oxide on the dielectric properties of biogenically synthesized ZnO nanoparticles. *Hybrid. Adv.* **3**, 100–109 (2023). <https://doi.org/10.1016/j.hybadv.2023.100059>
- Al-Farraj, E.S., Alhabarah, A.N., Ahmad, J., Al-Enizi, A.M., Naushad, M., Ubaidullah, M., Alshehri, S.M., Ruksana, T., Ahamad: Fabrication of hybrid nanocomposite derived from Chitosan as efficient electrode materials for supercapacitor. *Int. J. Biol. Macromol.* **120**, 2271–2278 (2018). <https://doi.org/10.1016/j.ijbiomac.2018.08.104>
- Alibwaini, Y.A., Hemeda, O., El-Shater, R., Sharshar, T., Ashour, A.H., Ajlouni, A.W., Arrasheed, E.A., Henaish, A.M.A.: Synthesis, characterizations, optical and photoluminescence properties of polymer blend PVA/PEO films doped eosin Y (EY) dye. *Opt. Mater. (Amst.)* **111** (2021). <https://doi.org/10.1016/j.optmat.2020.110600>
- Alshammari, F.H.: Physical characterization and dielectric properties of Chitosan incorporated by zinc oxide and graphene oxide nanoparticles prepared via laser ablation route. *J. Mater. Res. Technol.* **20**, 740–747 (2022). <https://doi.org/10.1016/j.jmrt.2022.07.046>
- Althubiti, N.A., Atta, A., Alotaibi, B.M., Abdelhamied, M.M.: Structural and dielectric properties of ion beam irradiated polymer/silver composite films. *Surf. Innov.* **11**, 90–100 (2022). <https://doi.org/10.1680/jstin.22.00010>
- Aparna, Nani, V., Manoj, B., Radhu, S.: Bandgap modification of graphene oxide in GO-silver nanocomposite (synthesized using tulsi and blueberry) as an alternative for fluorination. *Mater. Today Proc.* (2023). <https://doi.org/10.1016/j.matpr.2023.11.063>
- Basfer, N.M.: Enhancing Structural, Optical, and Thermal properties of PVA/PEO by incorporating CrBr2. *J. Non Cryst. Solids.* **621**, 122619 (2023). <https://doi.org/10.1016/j.jnoncrysol.2023.122619>
- Chiu, F.C., Chuang, Y.C., Liao, S.J., Chang, Y.H.: Comparison of PVDF/PVAc/GNP and PVDF/PVAc/CNT ternary nanocomposites: Enhanced thermal/electrical properties and rigidity. *Polym. Test.* **65**, 197–205 (2018). <https://doi.org/10.1016/j.polymertesting.2017.11.027>
- El Aassar, M.R., Sendi, R.K., Nuha, A.A., Harbi, A., Rabia, M.: Characterization and linear / nonlinear optical properties of PVA / CS / TiO₂ polymer nanocomposite films for optoelectronics applications. *Opt. Quantum Electron.* (2023). <https://doi.org/10.1007/s11082-023-05542-w>
- Elashmawi, I.S., Al-Muntaser, A.A.: Influence of Co3O4 nanoparticles on the Optical, and Electrical properties of CMC/PAM Polymer: Combined FTIR/DFT study. *J. Inorg. Organomet. Polym. Mater.* **31**, 2682–2690 (2021). <https://doi.org/10.1007/s10904-021-01956-9>

- Elashmawi, I.S., Menazea, A.A.: Different time's nd:YAG laser-irradiated PVA/Ag nanocomposites: Structural, optical, and electrical characterization. *J. Mater. Res. Technol.* **8**, 1944–1951 (2019). <https://doi.org/10.1016/j.jmrt.2019.01.011>
- Elashmawi, I.S., Abdelrazek, E.M., Hezma, A.M., Rajeh, A.: Modification and development of electrical and magnetic properties of PVA/PEO incorporated with MnCl₂. *Phys. B Condens. Matter.* **434**, 57–63 (2014). <https://doi.org/10.1016/j.physb.2013.10.038>
- Elashmawi, I.S., Alatawi, N.S., Elsayed, N.H.: Preparation and characterization of polymer nanocomposites based on PVDF/PVC doped with graphene nanoparticles. *Results Phys.* **7**, 636–640 (2017). <https://doi.org/10.1016/j.rinp.2017.01.022>
- Elashmawi, I.S., Al-Muntaser, A.A., Ismail, A.M.: Structural, optical, and dielectric modulus properties of PEO/PVA blend filled with metakaolin. *Opt. Mater. (Amst).* **126** (2022). <https://doi.org/10.1016/j.optmat.2022.112220>
- Elashmawi, I.S., Ismail, A.M., Abdelghany, A.M., Hegazi, M.M., Yassin, A.Y.: Electrical investigation and enhancement of optical, structural, and dielectric properties of flexible PVDF/LiZnVO₄ nanocomposites. *Discov Mater.* **3** (2023). <https://doi.org/10.1007/s43939-023-00053-7>
- Hameed, S.T., Qahtan, T.F., Abdelghany, A.M., Oraby, A.H.: Effect of zinc oxide nanoparticles on physical properties of carboxymethyl cellulose/ poly (ethylene oxide) matrix. *Phys. B Condens. Matter.* **633**, 413771 (2022). <https://doi.org/10.1016/j.physb.2022.413771>
- Hemalatha, K.S., Sriprakash, G., Ambika Prasad, M.V.N., Damle, R., Rukman, K.: Temperature dependent dielectric and conductivity studies of polyvinyl alcohol-ZnO nanocomposite film by impedance spectroscopy. *J. Appl. Phys.* **118** (2015). <https://doi.org/10.1063/1.4933286>
- Huang, T., chong Du, X., Duan, J., ling Xie, Y., Yang, J., Wang, Y.: Poly(ethylene oxide) induced microstructure and hydrolytic degradation behavior changes of poly(butylene sebacinate). *Polym. Test.* **61**, 8–16 (2017). <https://doi.org/10.1016/j.polymertesting.2017.05.001>
- Huang, X., Zhi, C., Lin, Y., Bao, H., Wu, G., Jiang, P., Mai, Y.V.: Thermal conductivity of graphene-based polymer nanocomposites. *Mater. Sci. Eng. R Reports.* **142**, 100577 (2020). <https://doi.org/10.1016/j.mser.2020.100577>
- Ibrahim, A.M.M., Abou Elfadl, A., El Sayed, A.M., Ibrahim, I.M.: Improving the optical, dielectric properties and antimicrobial activity of Chitosan-PEO-Gr-GO/MWCNTs: Nanocomposites for energy storage and food packaging applications. *Polym. (Guilf.)* **267**, 125650 (2023). <https://doi.org/10.1016/j.polymer.2022.125650>
- Menazea, A.A., Abdelbadie, S.A., Ahmed, M.K.: Manipulation of AgNPs coated on selenium/carbonated hydroxyapatite/ ϵ -polycaprolactone nanofibrous via pulsed laser deposition for wound healing applications. *Appl. Surf. Sci.* **508** (2020). <https://doi.org/10.1016/j.apsusc.2020.145299>
- Mousa, E.: On the electrical and optical properties of PVA for embedded electronics and optical applications. *J. Mater. Sci. Mater. Electron.* **33**, 20088–23106 (2022). <https://doi.org/10.1007/s10854-022-09075-y>
- Oh, J.Y., Kim, D.H., Bin Yang, J., Woon, J., Lee, D.W., Seo, D.S.: Graphene-oxide-doped oriented nickel oxide film achieved through brush coating for liquid crystal system. *Surf. Interfaces.* **43**, 103565 (2023). <https://doi.org/10.1016/j.surfin.2023.103565>
- Olabi, A.G., Abdokareem, M.A., Wilberforce, T., Sayed, E.T.: Application of graphene in energy storage device – A review, review. *Sustain. Energy Rev.* **135** (2021). <https://doi.org/10.1016/j.rser.2020.110026>
- Parvathi, E., Akshay, C.V., Dilraj, N., Arjun, G., Deepak, N.K.: Green synthesis of reduced graphene oxide by silolite. *Mater. Today Proc.* (2023). <https://doi.org/10.1016/j.matpr.2023.04.309>
- Raghuvanshi, S.K., Ahamad, B., Siddhartha, J.B.M., Krishna, A.K., Srivastava, M.A., Wahab, M.S., Khan: Effect of γ -irradiation on optical and chemical properties of CR-39 polymer. *Radiat. Eff. Defects Solids.* **167**, 764–781 (2012). <https://doi.org/10.1080/10420150.2011.653662>
- Sappan, Muthu, M., Stanly John Xavier, S., Ajith, P., Prem Anand, D.: Preparation and characterization studies of nano graphene oxide, *Mater. Today Proc.* **66** 2449–2454. (2022). <https://doi.org/10.1016/j.matpr.2022.06.367>
- Sharma, G., Thakur, B., Naushad, M., Kumar, A., Stadler, F.J., Alfadul, S.M., Mola, G.T.: Applications of Nanocomposite Hydrogels for Biomedical Engineering and Environmental Protection. Springer International Publishing (2018). <https://doi.org/10.1007/s10311-017-0671-x>
- Sreekanth, K., Siddaiah, T., Gopal, N.O., Madhava Kumar, Y., Ramu, C.: Optical and electrical conductivity studies of VO₂+doped polyvinyl pyrrolidone (PVP) polymer electrolytes. *J. Sci. Adv. Mater. Devices.* **4**, 230–236 (2019). <https://doi.org/10.1016/j.jsamd.2019.06.002>
- Tanaka, T., Montanari, G.C., Mülhaupt, R.: Polymer nanocomposites as dielectrics and electrical insulation-perspectives for processing technologies, material characterization and future applications. *IEEE Trans. Dielectr. Electr. Insul.* **11**, 763–784 (2004). <https://doi.org/10.1109/TDEI.2004.1349782>
- Zankana, M.M., Al-dalawy, S.M., Barzinjy, A.A.: Synthesis and characterization of bio-nanocomposites: Functionalization of graphene oxide with a biocompatible amino acid. *Hybrid. Adv.* **3**, 100070 (2023). <https://doi.org/10.1016/j.hybadv.2023.100070>

Zhou, T.N., Qi, X.D., Fu, Q.: The preparation of the poly(vinyl alcohol)/graphene nanocomposites with low percolation threshold and high electrical conductivity by using the large-area reduced graphene oxide sheets. *Express Polym. Lett.* **7**, 747–755 (2013). <https://doi.org/10.3144/expresspolymlett.2013.72>

Publisher's Note Springer Nature remains neutral with regard to jurisdictional claims in published maps and institutional affiliations.

Springer Nature or its licensor (e.g. a society or other partner) holds exclusive rights to this article under a publishing agreement with the author(s) or other rightsholder(s); author self-archiving of the accepted manuscript version of this article is solely governed by the terms of such publishing agreement and applicable law.

RETRACTED ARTICLE